THE JOURNAL OF BIOLOGICAL CHEMISTRY VOL. 284, NO. 52, pp. 36415–36423, DECEMBER 25, 2009

Glyphosate Resistance by Engineering the Flavoenzyme Glycine Oxidase*[S]

Received for publication, August 4, 2009, and in revised form, October 12, 2009 Published, JBC Papers in Press, October 28, 2009, DOI 10.1074/jbc.M109.051631

Mattia Pedotti[‡], Elena Rosini[‡], Gianluca Molla[‡], Tommaso Moschetti[§], Carmelinda Savino[¶], Beatrice Vallone[§], and Loredano Pollegioni[‡1]

From the [‡]Dipartimento di Biotecnologie e Scienze Molecolari and the Centro Interuniversitario di Ricerca in Biotecnologie Proteiche "The Protein Factory," Politecnico di Milano, Università degli Studi dell'Insubria, 21100 Varese, Italy, the [§]Department of Biochemical Sciences, "Sapienza," University of Rome, 00185 Rome, Italy, and the [¶]Consiglio Nazionale delle Richerche Institute of Molecular Biology and Pathology, 00185 Rome, Italy

Glycine oxidase from *Bacillus subtilis* is a homotetrameric flavoprotein of great potential biotechnological use because it catalyzes the oxidative deamination of various amines and D-isomer of amino acids to yield the corresponding α-keto acids, ammonia/amine, and hydrogen peroxide. Glyphosate (*N*-phosphonomethylglycine), a broad spectrum herbicide, is an interesting synthetic amino acid: this compound inhibits 5-enolpyruvylshikimate-3-phosphate synthase in the shikimate pathway, which is essential for the biosynthesis of aromatic amino acids in plants and certain bacteria. In recent years, transgenic crops resistant to glyphosate were mainly generated by overproducing the plant enzyme or by introducing a 5-enolpyruvylshikimate-3-phosphate synthase insensitive to this herbicide. In this work, we propose that the enzymatic oxidation of glyphosate could be an effective alternative to this important biotechnological process. To reach this goal, we used a rational design approach (together with site saturation mutagenesis) to generate a glycine oxidase variant more active on glyphosate than on the physiological substrate glycine. The glycine oxidase containing three point mutations (G51S/A54R/H244A) reaches an up to a 210-fold increase in catalytic efficiency and a 15,000-fold increase in the specificity constant (the k_{cat}/K_m ratio between glyphosate and glycine) as compared with wild-type glycine oxidase. The inspection of its three-dimensional structure shows that the α2-α3 loop (comprising residues 50–60 and containing two of the mutated residues) assumes a novel conformation and that the newly introduced residue Arg^{54} could be the key residue in stabilizing glyphosate binding and destabilizing glycine positioning in the binding site, thus increasing efficiency on the herbicide.

Glycine oxidase (GO)[2] from *Bacillus subtilis* (EC 1.4.3.19) is a flavoprotein oxidase consisting of four identical subunits; each subunit (≈42 kDa) contains one molecule of noncovalently bound FAD (1, 2). This enzyme catalyzes the oxidation of glycine in the biosynthesis of the thiazole ring of thiamine. Its crystal structure was solved as a complex with the inhibitor glycolate up to 1.8 Å resolution (3, 4). From a structural point of view, GO is classified as a member of the glutathione reductase family (subfamily GR_2); monomeric sarcosine oxidase and D-amino acid oxidase represent closer structural neighbors (4). GO and D-amino acid oxidase catalyze the oxidative deamination of amino acids to yield the corresponding α-imino acids and, after hydrolysis, α-keto acids, ammonia (or primary amines), and hydrogen peroxide (Scheme 1*a*), but they differ in substrate specificity. In addition to neutral D-amino acids (*e.g.* D-alanine and D-proline, which are also good substrates of D-amino acid oxidase), GO catalyzes the oxidation of primary and secondary amines (*e.g.* glycine, sarcosine) partially sharing substrate specificity with monomeric sarcosine oxidase (1, 2).

Glyphosate (*N*-phosphonomethylglycine), a broad spectrum herbicide, is an interesting synthetic amino acid. This dominant herbicide (almost 90% of crops worldwide) inhibits the monomeric enzyme 5-enolpyruvylshikimate-3-phosphate synthase (EPSPs), the penultimate step in the shikimate pathway, which is essential for the biosynthesis of aromatic amino acids in plants and certain bacteria. Glyphosate is a competitive inhibitor with respect to phosphoenolpyruvate of EPSPs, which is more effective on the plant enzyme with respect to the bacterial homologues. The details of the structure-function relationships in EPSPs from *Agrobacterium* sp. strain CP4 have also been elucidated (5). Its efficacy against all plant species, low cost, and low mammalian toxicity impact highly favor its use in crops that have a transgenic tolerance mechanism (6, 7). The currently commercially used glyphosate-resistant mechanisms are based on the overproduction of the plant enzyme (8) and on a transgene encoding a bacterial EPSPs that is insensitive to inhibition by glyphosate (6, 7). Most recently, a transgene encoding a soil microorganism glyphosate oxidoreductase that cleaves the nitrogen-carbon bond in glyphosate yielding aminomethylphosphonic acid (AMPA) and glyoxylate (9, 10) and the *N*-acetylation of the herbicide by an evolved bacterial acetyl-

* This work was supported by grants from the Fondo di Ateneo per la Ricerca (to L. P. and G. M.) and by the Consorzio Interuniversitario per le Biotecnologie and the Centro di Ricerca in Biotecnologie per la Salute Umana.

[S] The on-line version of this article (available at http://www.jbc.org) contains supplemental Table S1 and Fig. S1.

The atomic coordinates and structure factors (code 3IF9) have been deposited in the Protein Data Bank, Research Collaboratory for Structural Bioinformatics, Rutgers University, New Brunswick, NJ (http://www.rcsb.org/).

[1] To whom correspondence should be addressed: DBSM, Università degli studi dell'Insubria, via J. H. Dunant 3, Varese, Italy. Tel.: 332-421506; Fax: 0332-421500; E-mail: loredano.pollegioni@uninsubria.it.

[2] The abbreviations used are: GO, glycine oxidase; EPSPs, 5-enolpyruvylshikimate-3-phosphate synthase; AMPA, aminomethylphosphonate.

(a)

$$\text{E-FAD}_{ox} + \text{Gly} \rightleftharpoons \text{E-FAD}_{red} + NH_4^+ + \text{HCO-CO}_2\text{H (glyoxylate)}$$

$$\text{E-FAD}_{red} + O_2 \rightleftharpoons \text{E-FAD}_{ox} + H_2O_2$$

(b)

$$\text{E-FAD}_{ox} + \text{Glyphosate} \rightleftharpoons \text{E-FAD}_{red} + \text{NH}_2\text{-CH}_2\text{-PO}_3\text{H}_2 + \text{HCO-CO}_2\text{H (glyoxylate)}$$

aminomethylphosphonate (AMPA)

$$\text{E-FAD}_{red} + O_2 \rightleftharpoons \text{E-FAD}_{ox} + H_2O_2$$

(c)

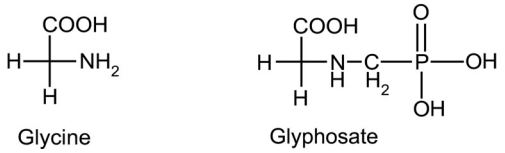

SCHEME 1. **Reaction catalyzed by GO on glycine (*a*) or on glyphosate (*b*) as substrate and structural comparison between glycine and glyphosate (*c*).**

transferase were proposed as further mechanisms for glyphosate tolerance in crops (11, 12). Currently, the only independent mechanism to give sufficient and stable resistance to glyphosate for commercialization of glyphosate-resistant crops has been glyphosate-resistant forms of EPSPs (10).

The investigation of the crystal structure and of the substrate specificity of GO prompted us to consider this flavoenzyme as a starting point for the evolution of new functions of biotechnological interest. In particular, we report here on a protein engineering study aimed to develop the activity of GO on glyphosate with respect to glycine (the physiological substrate). We thus propose that introducing the gene coding for the evolved GO in plants is an effective alternative mechanism for glyphosate tolerance in transgenic crops. In addition, transgenic plants that are able to oxidize glyphosate may represent an innovative bioremediation system for the soil treated with this herbicide.

EXPERIMENTAL PROCEDURES

Enzyme Expression and Purification—The pT7(ΔBH) expression plasmids (2) coding for His-tagged wild type and mutants of GO were transferred to the host BL21(DE3)pLysS *Escherichia coli* strain. Recombinant cells were grown at 37 °C in Terrific Broth medium containing 100 μg/ml ampicillin and 34 μg/ml chloramphenicol, and protein expression was induced in the exponential phase of growth by adding isopropyl β-D-1-thiogalactopyranoside to a final concentration of 0.5 mM. The cells were then grown at 30 °C and collected after ≈18 h by centrifugation. Crude extracts were prepared by sonication (four cycles of 30 s each) of the cell paste suspended with 50 mM disodium pyrophosphate buffer, pH 8.5, containing 5 mM EDTA, 2 μM FAD, 5 mM 2-mercaptoethanol, 0.7 μg/ml pepstatin, 1 mM phenylmethanesulfonyl fluoride, and 10 μg/ml deoxyribonuclease I (in a ratio of 2–3 ml of buffer/gram of *E. coli* cells). The insoluble fraction of the lysate was removed by centrifugation (2). The recombinant GO proteins were purified from the crude extracts by using HiTrap chelating affinity chromatography (GE Healthcare) as reported in (2, 13). The purified GOs were then equilibrated with 50 mM disodium pyrophosphate buffer, pH 8.5, and 10% glycerol (13).

Assay for GO Activity (and Substrate Specificity)—GO activity was assayed with an oxygen electrode on 10 mM glycine as substrate at pH 8.5 and 25 °C at air saturation ($[O_2]$ = 0.253 mM) (2). One unit of GO corresponds to the amount of enzyme that consumes 1 μmol of oxygen/min at 25 °C. Substrate specificity of GO was investigated on different compounds as substrate by two different methods: an oxygen consumption amperometric assay, as described above, and spectrophotometric determination of the hydrogen peroxide produced by the GO reaction. This latter assay was performed using a microtiter plate; each well contained 100 μl of 90 mM substrate solution, 0.32 mg/ml *o*-dianisidine, and 1 unit/ml of horseradish peroxidase in 100 mM disodium pyrophosphate buffer, pH 8.5. The increase in absorbance at 450 nm was followed by using a Biotrak II plate reader (GE Healthcare) (2).

Reaction Product Analysis—To study the reaction catalyzed by GO on glyphosate, the products formed during the reaction with 5 mM of the herbicide were analyzed using different methods. α-Keto acid production was estimated as the production of 2,4-dinitrophenylhydrazone derivatives by a reaction with 2,4-dinitrophenylhydrazine; calibration curves were achieved using both glyoxylate and pyruvate, because the corresponding α-keto acid derivatives show different absorbance spectra and extinction coefficients (1). To assess the production of formaldehyde, the GO reaction was coupled to the formaldehyde dehydrogenase NAD-dependent reaction following the production of NADH at 340 nm; a calibration curve was assessed using formaldehyde, and blank reactions contained all of the assay components except GO or glyphosate (1). Molecular oxygen consumption and H_2O_2 production were determined using the methods described above. AMPA was determined by electrospray ionization mass spectrometry; the spectra were collected on a Bruker Esquire 3000+ with quadrupole ion trap detector. The solution was transferred into the ion source via microsyringe at a flow rate of 4 μl/min. N_2 flow was 10 liters/min at 250 °C.

Molecular Modeling Studies—Automated ligand docking was performed by Autodock 4.0, a package based on a Montecarlo simulated annealing approach (14). The three-dimensional structure of the substrate glyphosate was generated using the PRODRG2 server (15). Swiss PDBviewer 3.7 was used to build three-dimensional models of GO variants and VMD 1.8.6 to visualize the three-dimensional protein structure.

Site-directed and Site Saturation Mutagenesis—Single-point mutations were generated by site-directed mutagenesis using the QuikChange site-directed mutagenesis kit (Stratagene, La Jolla, CA) and the GO cDNA subcloned into the pT7(ΔBH)-HisGO plasmid (13). The introduction of the desired mutations was confirmed by automated DNA sequencing. Site saturation mutagenesis was carried out at different amino acid positions

by using the same procedure as for site-directed mutagenesis and a set of degenerated synthetic oligonucleotides (16); the PCR products were used to transform JM109 *E. coli* cells. Subsequently, the recombinant plasmids were transferred to BL21(DE3)pLysS *E. coli* cells, and these clones were used for the screening procedure.

Screening for Evolved GO Variants—The mutant libraries obtained from site saturation mutagenesis were screened by means of a rapid colorimetric assay based on the determination of hydrogen peroxide produced by single recombinant *E. coli* cultures (1 ml) grown to saturation in Luria Bertani medium to which 0.5 mM isopropyl β-D-1-thiogalactopyranoside was added and then incubated at 30 °C for 5 h. An aliquot (100 μl) of each culture was transferred to two wells of a microtiter plate; 100 μl of lysis buffer (50 mM disodium pyrophosphate buffer, pH 8.5, 1 mM EDTA, 100 mM NaCl, 20% cell lytic (Sigma-Aldrich) and 1 mg/ml deoxyribonuclease I) were added, and the cells were incubated at 37 °C for 30 min. The oxidase activity was assayed on the crude extracts (200 μl) by adding 100 μl of 18 mM glyphosate or 1.8 mM glycine, 0.2% Triton X-100, 0.3 mg/ml *o*-dianisidine, and 1 unit/ml horseradish peroxidase in 100 mM disodium pyrophosphate buffer, pH 8.5. The time course of the absorbance change at 450 nm was followed at room temperature and compared with that of control cells (expressing wild-type GO or lacking the GO-encoding plasmid). Each clone was evaluated in three independent trials, and the average response was calculated; the clones that outperformed the control were selected for further analysis and biochemical characterization.

Enzyme Characterization—The kinetic parameters of wild-type GO and variants were determined using a fixed amount of enzyme and different substrate concentrations (glycine, 0–500 mM; glyphosate, 0–800 mM). Activity was assayed using the oxygen consumption assay at 21% oxygen saturation as described above (2).

Spectral experiments were carried out at 15 °C in 50 mM disodium pyrophosphate buffer, pH 8.5, 10% glycerol. Extinction coefficients of the GO variants were determined by heat denaturation (at 95 °C for 10 min) or by SDS denaturation (final concentration, 1%) of the enzymes and using the absorption coefficient for free FAD of 11.3 mM^{-1} cm^{-1}.

The stability of GO (wild-type and variant) was determined by temperature ramp experiments measuring protein and flavin fluorescence changes with a Jasco FP-750 spectrofluorimeter equipped with a thermostatted cell holder and using a 3-ml cuvette. The experiments were performed using a software-driven, Peltier-based temperature controller, which allowed a temperature gradient of 0.5 °C/min (17). Fixed wavelength measurements were taken at 340 nm (excitation wavelength, 298 nm) and 526 nm (excitation wavelength, 455 nm) for tryptophan and flavin fluorescence, respectively. The denaturation curve was used to extrapolate the melting temperature (T_m value) of the enzymes, as described in Ref. 17.

Crystallization and Data Collection—The structure of the G51S/A54R/H244A GO was determined in the form bound with the inhibitor glycolate, given the failure to grow cocrystals in the presence of glyphosate or to introduce it into pregrown variant GO crystals by soaking. Crystals of G51S/A54R/H244A GO were grown in a 1:1 mixture of protein (10 mg/ml in 186 mM Na-Hepes, pH 8.1, 3% glycerol) and crystallization solution (100 mM Na-Hepes, pH 7.5, 28% (w/v) polyethylene glycol 400, 200 mM calcium chloride, 30 mM sodium glycolate) at 20 °C according to the hanging drop method; they were 100 × 25 × 25 μm in size. The crystals grew within 1 week and were frozen in liquid N_2 without adding any cryoprotectant. X-ray diffraction data were collected at 100 K at the BESSY, BL14.2 (Berlin, Germany; detector MX225 ccd; x-ray wavelength, 1.04063 Å).

TABLE 1

Crystallographic data collection and refinement statistics for G51S/A54R/H244A GO

The values for the highest resolution shell are shown in parentheses. Wavelength of data collection, temperature, and beamline are given under "Experimental Procedures."

	G51S/A54R/H244A mutant GO
Data collection	
Space group	$C\,2\,2\,2_1$
a, *b*, *c* (Å)	72.34, 214.78, 216.90
α, β, γ (°)	90, 90, 90
Resolution range (Å)	76.25–2.60 (2.74–2.60)
Completeness (%)	100 (100)
Redundancy (%)	10.1 (10.1)
R_{meas}	0.09 (0.36)
$<I/\sigma I>$	22.7 (10.7)
Refinement	
Resolution (Å)	2.60
No. of reflections	49,195
R_{cryst}/R_{free} (%)	19.6/25.6
No. of protein atoms	11731
No. of ligand atoms (FAD and glycolate)	232
No. of water atoms	166
B-factors (Å²)	
Protein	31.16
Ligand	33.52
Water	26.27
Overall	43.99
Root mean square deviations	
Bond lengths (Å)	0.010
Bond angles (°)	1.308
Ramachandran (%)	
Most favored/allowed/generous/disallowed	88.3/11.4/0.2/0.1

The data were indexed, integrated, and scaled by using MOSFLM and SCALA (18). The CCP4 program suite (19) was used to subsequently evaluate the data and refine the structure (Table 1). Unit cell dimensions were isomorphous with those previously measured (4). The initial phases were derived from the deposited structure (Protein Data Bank code 1RYI) (4). The model was subjected to iterative rounds of refinement and model building. For refinement, Refmac5 in CCP4 was employed (20); then the model was adjusted, and water was added with COOT (21). The quality of the final model was analyzed by using PROCHECK (22); only one residue was found to be in the disallowed region of the Ramachandran plot, *i.e.* Arg^{179} in chain A, as also observed for the wild-type GO (Protein Data Bank code 1RYI) (4).

In analogy to what was reported for wild-type GO (4), the final model of G51S/A54R/H244A variant does not contain the 13 additional residues at the N terminus (MHHHHHH-MARIRA) and the residues Glu^{365}–Ile^{369} at the C terminus. Moreover, the region corresponding to Arg^{54}–Asp^{60} showed poor electron density for this protein, too. Thus, we could only model the whole sequence for chain A, because the other chains displayed no electron density for the following residues: chain

B, residue 56; chain C, residues 55–57; and chain D, residues 54–56. The coordinates were deposited at the Protein Data Bank with accession number 3IF9.

RESULTS

Substrate Specificity and Products of Glyphosate Oxidation—Wild-type GO shows a similar specific activity on sarcosine and glycine (1.0 and 0.8 units/mg of protein, respectively), and it is known to act on different amines and D-amino acids (2). The activity of wild-type GO was determined on several compounds using the peroxidase/*o*-dianisidine spectrophotometric assay at a fixed (90 mM) substrate concentration on a microtiter plate. The results, reported as a percentage with respect to the absorbance change with sarcosine (=100%), confirm the wide substrate specificity of wild-type GO (Fig. 1); in addition to sarcosine and glycine, even ethylglycine ester, D-2-aminobutyrate, *N*-methyl-D-alanine, and the herbicide glyphosate are oxidized by GO. The apparent kinetic parameters were then determined on glyphosate using the oxygen consumption assay at 21% oxygen saturation and compared with those measured on glycine. The specific activity value is similar to that for glycine (1.3 units/mg of protein *versus* 0.8 unit/mg of protein), but a significantly higher $K_{m,app}$ (87 mM *versus* 0.7 mM) is evident. The specificity constant (the k_{cat}/K_m ratio between glyphosate and glycine; see last column in Table 2) (16) is ≈0.01, thus indicating the low kinetic efficiency of wild-type GO for the herbicide glyphosate.

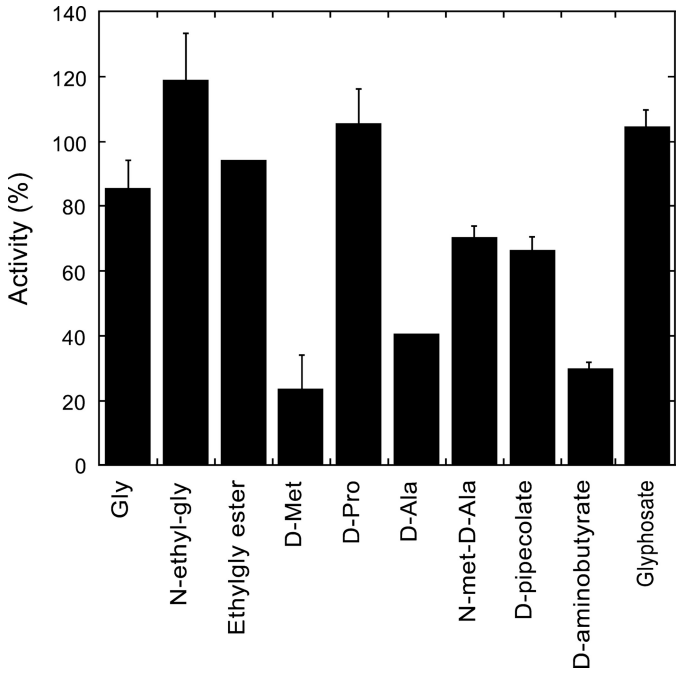

FIGURE 1. **Assay of GO activity on various compounds using the peroxidase/*o*-dianisidine coupled assay.** The values are reported as percentages of the absorbance change at 450 nm measured with sarcosine as substrate (taken as 100%). The data are reported ± S.D. for three measurements.

Following the addition of GO to a solution containing 5 mM glyphosate in the chamber of an oxymeter, a decrease in the oxygen concentration is evident; addition of catalase halved the slope of oxygen consumption, indicating that hydrogen peroxide is the product of oxygen reduction. This is also confirmed by the spectrophotometric assay coupled with horseradish peroxidase and *o*-dianisidine. The GO reaction on glyphosate produces glyoxylate as keto acid, as made evident by the spectrum of the corresponding phenylhydrazone derivative (1), whereas no formaldehyde is produced (no reaction is observed using the formaldehyde dehydrogenase-coupled assay). Notably, the amount of produced glyoxylate stoichiometrically corresponds to the amount of oxygen consumed as well as the rate of formation (not shown). Finally, the reaction solution was directly infused in the electrospray ionization source, and the full scan mass spectrum was acquired. The negative ion polarity spectrum showed a significant peak at *m*/*z* 110, consistent with deprotonated AMPA. The assignment was confirmed by enrichment of the solution in standard AMPA. A summary of the reaction catalyzed by GO on glyphosate is reported in Scheme 1*b*, which represents the typical reaction of a deaminating oxidase (the same results have been obtained using the evolved GO; see below). Even though two reaction products of glyphosate oxidation (*i.e.* glyoxylate and AMPA) are produced by both GO and glyphosate oxidoreductase, the two flavoenzymes catalyze a different overall reaction because of hydrogen peroxide production by GO (which is not produced by the oxidoreductase) and the use of 1 mol of oxygen/1 mol of glyphosate *versus* 0.5 O_2/glyphosate consumed by glyphosate oxidoreductase (9, 10).

Docking Analysis—The binding mode of glyphosate in the GO active site was simulated using Autodock 4.0 software (14). In the best solutions (the ones possessing the lowest energy), glyphosate perfectly matches in GO active site and is bound in the same orientation inferred for typical substrates (Fig. 2) (3, 4). Glyphosate is correctly positioned for catalysis because its C-α is over the nitrogen (5) of the isoalloxazine ring of the

TABLE 2

Comparison of the apparent kinetics parameters on glycine and glyphosate determined for wild-type and variants of GO obtained by site saturation mutagenesis of the positions identified by docking analysis or by introducing multiple mutations, as suggested by site saturation mutagenesis results

	Glycine		Glyphosate		$k_{cat,app}/K_{m,app}$ of glyphosate
	$k_{cat,app}$	$K_{m,app}$	$k_{cat,app}$	$K_{m,app}$	$k_{cat,app}/K_{m,app}$ of glycine
	s^{-1}	mM	s^{-1}	mM	
Wild type	0.60 ± 0.03	0.7 ± 0.1	0.91 ± 0.04	87 ± 5	0.01
H244A	0.63 ± 0.06	1.5 ± 0.3	0.77 ± 0.03	78 ± 4	0.02
Y241H	0.91 ± 0.05	38 ± 3	1.30 ± 0.03	41 ± 3	1.0
A54R	1.2 ± 0.1	28 ± 3	1.50 ± 0.02	4.4 ± 0.3	8.5
G51R	0.35 ± 0.02	53 ± 8	1.8 ± 0.1	6.5 ± 0.7	40
G51R/A54R	0.70 ± 0.03	59 ± 4	0.70 ± 0.03	1.0 ± 0.1	58
G51S/A54R	0.91 ± 0.02	35 ± 1	1.05 ± 0.05	1.3 ± 0.1	31
G51S/A54R/H244A	1.5 ± 0.1	105 ± 11	1.05 ± 0.05	0.5 ± 0.03	150

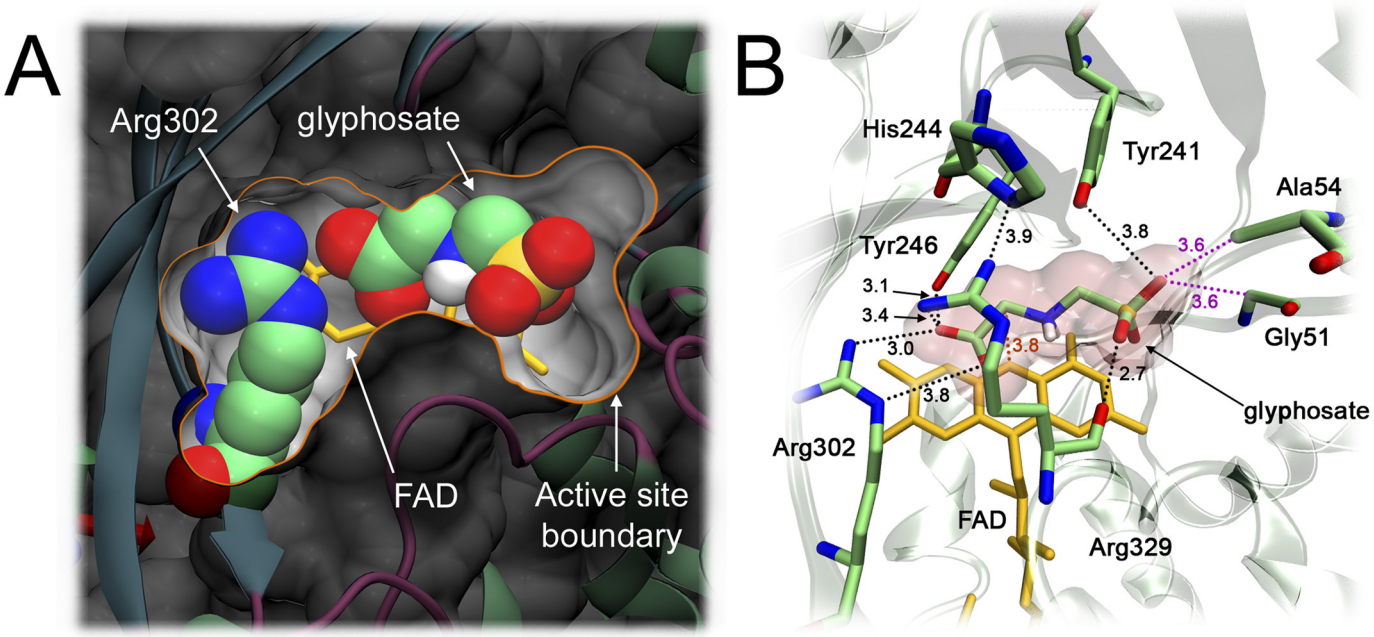

FIGURE 2. *A*, cross-section of GO showing the positioning of glyphosate in the active site and its interaction with Arg^{302} as indicated by docking analysis. The accessible space of the active site is shown in *light gray*; molecules are displayed by van der Waal's representation. *B*, model of GO active site in complex with the substrate glyphosate. The figure shows the main residues (with the relative distances) that interact with glyphosate. The docking of the ligand was predicted by docking analysis using the program AutoDock 4.0, and the model was developed using Swiss PDBviewer 3.7. The crystal structure of GO in complex with glycolate (Protein Data Bank code 1RYI) was used as starting structure.

cofactor (distance, ≈3.4 Å), the correct position for hydride transfer. The carboxylic group of the herbicide interacts via a double bridge to the Arg^{302} side chain and the phosphonate, pointing toward the active site entrance, might form H-bonds with Gly^{51} (3.6 Å) and Ala^{54} (3.6 Å) backbones and Tyr^{241} (3.8 Å) and Arg^{329} (3.4 Å) side chains. In addition to the residues reported above, the docking model of the GO-glyphosate complex identified further protein residues that could modulate the affinity for the substrate (Fig. 2*B*).

Selection of GO Variants Obtained by Site Saturation Mutagenesis—On the basis of the *in silico* analysis, site saturation mutagenesis was independently performed at positions Met^{49}, Gly^{51}, Ala^{54}, Met^{95}, Tyr^{241}, His^{244}, Tyr^{246}, Met^{261}, Arg^{302}, Arg^{329}, and Asn^{330} using the QuikChange kit and the wild-type GO cDNA as template. The activity of GO variants was screened on a microtiter plate using the peroxidase/*o*-dianisidine spectrophotometric assay. For each position, up to 200–250 clones were screened, giving a 96% probability that every single amino acid is introduced at the desired position (16). The clones most active on glyphosate as identified through the screening procedure (Fig. 3) were isolated, and the substitutions were identified by automatic DNA sequencing. These GOs were expressed in *E. coli* cells and purified by HiTrap chelating chromatography (≈90% purity). All of the variants show a lower expression yield than the wild-type GO (in terms of purified protein/liter of fermentation broth; supplemental Table S1), the only exception being H244A, whose production level is 2-fold higher. It is noteworthy that the substitution of Arg^{302} is associated with the complete abolition of enzymatic activity (data not shown), thus confirming a primary role for this residue in substrate binding (4).

All of the enzyme variants exhibited a hyperbolic substrate saturation for both glyphosate and glycine. Comparison of the

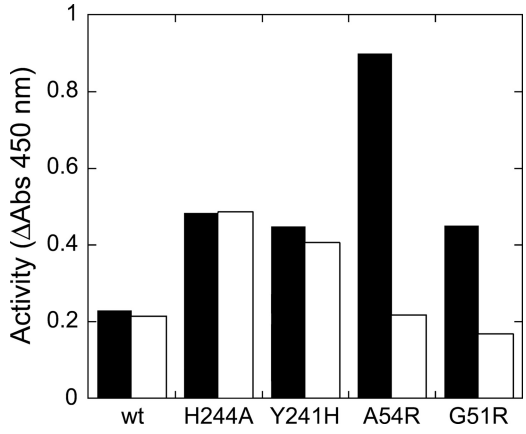

FIGURE 3. **Screening response of BL21(DE3)pLysS *E. coli* recombinant clones expressing wild type (*wt*) and the best four single point GO variants as obtained by site saturation mutagenesis experiments.** The activity is reported as absorbance change at 450 nm with 18 mM glyphosate (*black*) or 1.8 mM glycine (*gray*) as substrate after ≈18 h of incubation (see "Experimental Procedures" for details).

kinetic parameters of wild type and variants of GO indicates that the increase in kinetic efficiency on glyphosate is mainly caused by a dramatic decrease in $K_{m,app}$ (up to 20-fold for the A54R enzyme); analogously, the decrease in kinetic efficiency on glycine is mainly due to an increase in the $K_{m,app}$ parameter (Table 2). For both substrates, changes in the $k_{cat,app}$ parameters are less pronounced (≤2-fold). These alterations in kinetic properties result in a GO variant (G51R) with a 4000-fold increase in the specificity constant as compared with the wild-type enzyme (from 0.01 up to 40; see the last column of Table 2).

Introduction of Multiple Mutations—The single-point GO variants obtained by site saturation mutagenesis and having improved kinetic efficiency on glyphosate were used as a start-

TABLE 3

Comparison of T_m values for unfolding of wild-type and evolved variants of GO as determined by following protein and flavin fluorescence changes during temperature ramp experiments

The fluorescence experiments were performed in 50 mM disodium pyrophosphate, pH 8.5, 10% glycerol at an identical heating rate (0.5 °C/min). The protein concentration was 0.1 mg/ml in all measurements.

	T_m (°C)	
	Trp fluorescence	FAD fluorescence
Wild type	56.9 ± 0.1	58.7 ± 0.2
A54R	44.8 ± 0.3	46.6 ± 0.9
G51R	41.3 ± 0.6	42.8 ± 0.1
G51R/A54R	34.7 ± 0.7	35.1 ± 1.1
G51S/A54R	45.3 ± 0.2	46.9 ± 0.2
G51S/A54R/H244A	45.7 ± 1.0	45.1 ± 0.2

ing point for producing enzyme variants containing multiple mutations. The kinetics results suggest that positions 51 and 54 play a main role in GO affinity for glyphosate (Table 2). Therefore, the best mutations were combined, and site saturation mutagenesis of position 51 was carried out using the cDNA encoding for the A54R GO as a template and further introducing the H244A mutation that increases the protein expression (supplemental Table S1). From the screening procedure the G51S/A54R/H244A GO variant was identified. This evolved enzyme exhibits a 210-fold increase in the catalytic efficiency on glyphosate and a 15,000-fold increase in the specificity constant as compared with wild-type GO (Table 2), forming the basis for an effective system for glyphosate degradation.

General Properties of GO Variants—The visible absorbance spectra of GO purified variants in the oxidized state are similar to that of the wild-type enzyme in all cases (not shown); the estimated flavin absorption coefficient of the main peak at ≈455 nm is between 11.3 and 13.1 mM^{-1} cm^{-1} (supplemental Table S1). Denaturation experiments of GO variants show that the flavin cofactor is not covalently bound to the apoprotein moiety (after denaturation and centrifugation the protein pellets are colorless), analogously to the wild-type flavoenzyme (1, 2). Similarly, substitutions introduced in the evolved GO variants do not affect the content in secondary and tertiary structure as made evident by comparing their near- and far-UV CD spectra (not shown). The only exception is the G51R/A54R variant, which shows a lower amount of secondary structure than and an altered tertiary structure from wild-type GO (lower intensity of the CD signal at ≈280 nm and a 2-fold higher flavin fluorescence).

To compare the temperature sensitivity of wild-type GO and its more interesting variants, temperature ramp experiments were performed in which both protein and flavin fluorescence was detected as probes of protein (un)folding (17). For all of the variants analyzed, the midpoint transition temperature (T_m) decreases in comparison with wild-type GO (Table 3). A significantly lower stability at room temperature is evident for G51R/A54R GO (its activity is fully lost after 50 h), whereas the A54R, G51S/A54R, and G51S/A54R/H244A variants show time courses of inactivation at 25 °C similar to that of wild-type GO, *i.e.* 72 ± 10% *versus* 80 ± 9% of residual activity after 30 h and 60 ± 5% *versus* 70 ± 10% after 72 h of incubation for these variants and wild-type GO, respectively.

Structural Overview of G51S/A54R/H244A GO—The structure of the evolved G51S/A54R/H244A GO was determined in complex with glycolate at 2.6 Å resolution, and it was isomorphous with wild-type GO; no significant changes were observed either in the quaternary assembly of the enzyme or in its tertiary fold. In addition, the specific contacts that pertain to binding of FAD were not modified, nor was the overall architecture of the active site (see below). Superposition of GO wild-type and G51S/A54R/H244A variant structures yields a root mean square deviation between the main chain and side chain atoms of 0.39 and 0.88 Å, respectively. The overall variations are within the values expected from two independent determinations of the same structure, but a significant alteration was observed in the loop connecting α-helices 2 and 3 (loop α2-α3, comprising residues 50–60), which is on top of the active site (3, 4). Two of the mutations introduced into G51S/A54R/H244A GO are located on the α2-α3 loop, and Ala^{244}, the third substitution, is the tip of a β-hairpin (connecting β-strands 12 and 13) directly facing the loop. This loop has already been described as a mobile element within the GO tetramer (3, 4); it is neither involved in protein-protein interaction nor engaged in crystal contacts, whereas it seems to change its conformation according to the presence and the nature of the ligand in the binding site. Indeed, the thermal B factor shows a peak in the region 50–60 of all monomers of the asymmetric unit in all reported GO structures (3, 4), thus confirming its enhanced mobility (supplemental Fig. S1). Interestingly, in the GO homologue monomeric sarcosine oxidase, too, the corresponding loop is a mobile region, which has been proposed to regulate the accessibility of the active site (4, 23).

Concerning the active site geometry, the residues Arg^{302} and Met^{49} maintain their position, whereas a moderate change was observed for Tyr^{241} and Arg^{329} (Fig. 4). This is due to the close A54R mutation because the long side chain of the newly introduced arginine causes a slight lifting of Tyr^{241} from the binding site that results in a 1.03 Å displacement of its hydroxyl group and a 0.53 Å displacement of the Cγ of Arg329 (Fig. 4*A*). Because of the high degree of flexibility of the α2-α3 loop, the residues cannot be unambiguously positioned in three protomers of the GO tetramer, but at least in monomer A, we were able to trace and fit the loop within the electron density. Clearly this loop in the G51S/A54R/H244A variant assumes a position that does not correspond to the one found in the wild-type GO structure (Fig. 4*B*). The major displacement is observed for Glu^{55} and Cys^{56} (4.7 and 4.6 Å, respectively, for the Cα atoms), whereas the positions of G51S and A54R Cα are unmodified (apart from a 0.6 Å shift of the Cα of Ser^{51}; see supplemental Fig. S1). The main reason for this rearrangement seems to reside in the bulk introduced by the side chain of Arg^{54}, which points into the active site and forces the loop to assume a different configuration.

We modeled glyphosate in the active site of the G51S/A54R/H244A variant in the same position as identified for wild-type GO in docking analyses (Fig. 4*B*). Consistently with the conservation of the main binding site features, the carboxylate group of glyphosate still establishes favorable electrostatic interactions and hydrogen bonds with Arg^{329} and Tyr^{246}. In any case, the serine introduced at position 51 (instead of a glycine) is at the appropriate distance to interact with the phosphonate group of glyphosate, as does Arg^{54} also. The side chain of Arg^{54}

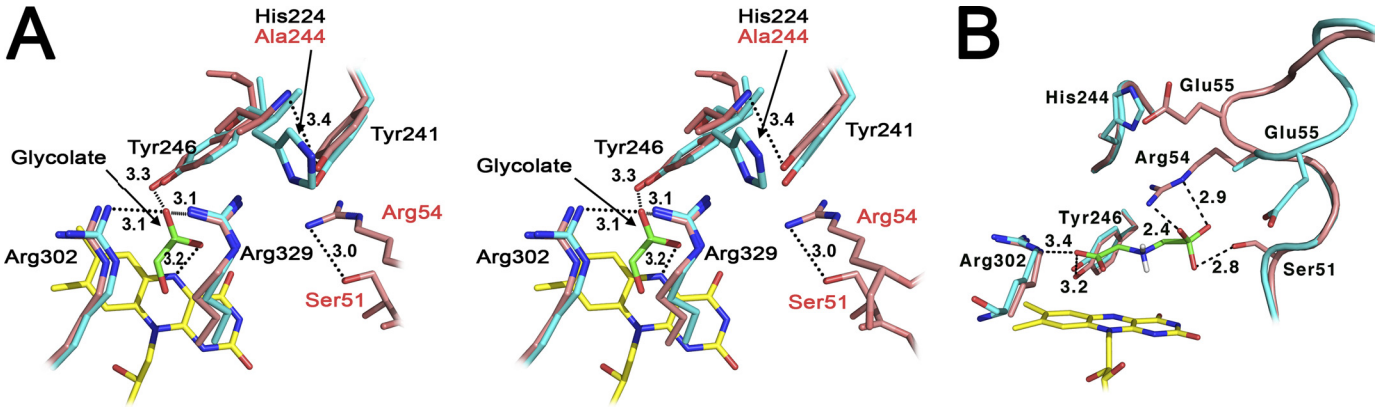

FIGURE 4. **Superposition of the active site of wild-type (*cyan*, Protein Data Bank code 1RYI) and monomer A of G51S/A54R/H244A (*pink*, Protein Data Bank code 3IF9) GOs.** *A*, stereo view showing the overlay of the active site side chains involved in interaction with the ligand glycolate (*green*), as discussed in the text. *B*, superposition of wild-type and G51S/A54R/H244A GO structures showing the different conformation of the main chain of α2-α3 loop (on the *right*). The ligand glyphosate (*green*) is positioned according to the docking analysis to wild-type GO (see also Fig. 2). For the sake of clarity, only the FAD and the ligand belonging to the wild-type GO structure are shown, and Arg^{329} was omitted in *B*. Distances (in Å) for interactions are shown in *black*, and the isoalloxazine ring of FAD is in *yellow*. The figure was prepared with PyMol (26).

is very mobile; we observed that this latter residue points inside the binding site, but the exact position of its guanidinium group in the variant GO-glyphosate complex is unknown. Bearing this *caveat* in mind, we have observed that: (i) the guanidinium group of Arg^{54} establishes favorable electrostatic interactions with the phosphonate group of glyphosate in our model; (ii) the arginine side chain, given the conformation assumed by the α2-α3 loop, displaces the side chain of Glu^{55} that points away from the active site in the G51S/A54R/H244A variant. Bearing in mind that, in wild-type GO bound to acetylglycine, Glu^{55} in conjunction with Arg^{329} forms a lid that shelters the ligand from the bulk solvent (3), it is clear that the presence of Arg^{54} would disrupt this interaction by displacing Glu^{55}. On the other hand, once glyphosate is bound, Arg^{54} interacts with the phosphonate group, contributing to its stabilization. The introduction of an arginine at position 54, as also made evident from characterization of the single point variants, together with the displacement of the negative charge of Glu^{55} has the effect of enhancing the affinity for glyphosate as well as of decreasing that for glycine.

The role of the H244A mutation cannot be rationalized in a straightforward manner. Previous site-directed mutagenesis studies show that the substitution of His^{244} significantly affects the rate of flavin reduction with sarcosine as substrate (from 170 for wild type to 8 s^{-1} for H244F GO), even if this change does not alter the turnover number (13). Substituting His^{244} with a shorter alanine residue would facilitate the remodeling of the active site following the attainment of a new conformation for the α2-α3 loop in the variant GO, in particular avoiding a clash with Glu^{55} while facilitating the interaction of Arg^{54} with the phosphonate group of glyphosate.

DISCUSSION

In this paper, we describe the evolution of *B. subtilis* glycine oxidase to obtain an enzyme with a high catalytic efficiency on the herbicide glyphosate. First, we analyzed the substrate preference of wild-type GO, highlighting its wide substrate specificity (Fig. 1). We also demonstrated that wild-type GO oxidizes the herbicide glyphosate, which is a synthetic amino acid largely used in agriculture and which presents structural features similar to those of glycine (Scheme 1*c*). GO catalyzes the deaminative oxidation of glyphosate because it yields glyoxylate, AMPA, and hydrogen peroxide using 1 mol of dioxygen/1 mol of herbicide (Scheme 1*b*). This reaction differs from that of glyphosate oxidoreductase because of a stoichiometry of two molecules of glyphosate oxidized per molecule of oxygen and the lack of hydrogen peroxide production (9, 10). Furthermore, the mechanism proposed for the oxidoreductase in which the reduced flavin obtained by oxidation of the first molecule of glyphosate catalyzes the oxygenation of a second molecule of glyphosate is profoundly different from the hydride transfer mechanism proposed for GO (3, 4).

The efficient oxidation of glyphosate by wild-type GO is limited by the low apparent affinity ($K_{m,app}$ = ≈90 mM; Table 2). To understand the putative mode of glyphosate binding at the GO active site, an *in silico* molecular docking analysis was carried out. In the best solutions glyphosate is bound in the same orientation inferred for its natural substrate glycine and with the phosphonate moiety pointing toward the entrance of the active site. The docking analysis identified the residues potentially involved in glyphosate binding (Fig. 2*B*). A number of GO variants with improved activity on glyphosate were recognized after site saturation mutagenesis on 11 positions of the active site. Finally, we combined the information gathered from the site saturation mutagenesis approach, producing a GO variant containing multiple mutations (G51S/A54R/H244A) and possessing an apparent specificity constant (the ratio between k_{cat}/K_m for the glyphosate and glycine) up to 15,000-fold higher than that for the wild-type enzyme. A total of three amino acid replacements introduced into wild-type GO suffice to provide a 13.2 kJ/mol decrease in the free energy of activation for the reaction on glyphosate and a 11.1 kJ/mol increase of the same value for the oxidation of glycine ($\Delta\Delta G$ values were calculated from the data in Table 2).

The crystal structure of the best GO variant in complex with glycolate enables us to pinpoint structural features that affect the evolution of its substrate preference. The substitutions

introduced in the evolved G51S/A54R/H244A GO appear to modify its substrate preference acting in different ways: (i) The α2-α3 loop (comprising residues 50–60 and possessing a high mobility) assumes a different conformation in the G51S/A54R/H244A variant as compared with wild-type GO. This rearrangement is mainly due to the introduction of the bulky side chain of arginine at position 54, which appears to locate close to the phosphonate group of glyphosate. This mutation replaces a neutral residue with a positively charged amino acid; new electrostatic interactions in G51S/A54R/H244A GO allow a tighter binding of the herbicide, maintaining the optimal positioning for catalysis (Fig. 4*B*). (ii) The introduction of arginine residue(s) at the active site entrance (positions 51 and 54) improves the kinetic efficiency of GO on glyphosate by decreasing the $K_{m,app}$ value (up to 20-fold in the G51R/A54R GO), whereas the maximal activity was only slightly affected (maximal change was a 2-fold increase in the G51R variant compared with the wild-type GO; Table 2). On the other hand, this substitution(s) negatively affects the protein stability; the G51R/A54R double variant shows a drastically lower stability than the wild type, and the other evolved GO variants (its activity is fully lost after 50 h of incubation at room temperature; Table 3), thus limiting its biotechnological use. Instead, the G51S/A54R/H244A GO shows stability, which is suitable for its utilization at room temperature; 60 and 70% of residual activity after 3 days at room temperature was measured for this variant and wild-type GO, respectively. (iii) The dramatic increase in specificity constant observed for the best GO variant is also due to the decrease in kinetic efficiency on glycine. This effect, too, is mainly due to a decrease in binding energy ($K_{m,app}$ for glycine is ≈150-fold higher in G51S/A54R/H244A than for the wild-type GO), whereas the maximal activity on glycine is only marginally altered in the evolved GO variants (Table 2). (iv) The presence of an alanine residue at position 244 only marginally affects the kinetic properties of GO when it is the only mutation introduced in the protein, but it had a synergistic effect both on the activity on glyphosate as substrate (Table 2) and the level of protein expression (supplemental Table S1) when it is introduced in the G51S/A54R GO. It appears that the smaller alanine residue at position 244 eliminates steric clashes with Glu^{55}, for example, thus facilitating the interaction between Arg^{54} and glyphosate in the evolved GO variants.

The observation that the same products are produced by glyphosate oxidation using GO and glyphosate oxidoreductase (*i.e.* AMPA and glyoxylate) might suggest a close similarity between these two FAD-containing flavoenzymes. The reaction catalyzed by the two enzymes strongly differs concerning the oxygen utilization and hydrogen peroxide production. Furthermore, the two enzymes show a low sequence identity (18.1%); a Blast analysis identifies a number of D-amino acid dehydrogenase as the most related proteins for glyphosate oxidoreductase. A further main difference is related to the kinetic properties of the two glyphosate-converting enzymes; although the apparent maximal activity reported for glyphosate oxidoreductase is not easily comparable with the value determined for GO (it was measured at higher temperature and on crude extracts, determining the amount of enzyme by means of Western blot analysis), the evolved GO we describe here shows a 5-fold lower K_m for glyphosate and a kinetic efficiency (k_{cat}/K_m ratio) 1 order of magnitude higher than that of the best variant obtained for glyphosate oxidoreductase (2.1 *versus* 0.3 mM^{-1} s^{-1}, respectively) (9, 10). This higher catalytic efficiency is most apparent when comparing recombinant proteins expressed in *E. coli*. The specific activity in the crude extract of the evolved GO described here is 20 milliunits/mg of protein, whereas that for glyphosate oxidoreductase is ≤0.015 milliunit/mg of protein. The low level of activity observed for the oxidoreductase might explain the limitations encountered to develop commercially available crops based on this enzyme. Concerning the toxicity of GO-produced glyphosate products, AMPA has been shown to be mildly toxic to soybean (24, 25); this potential for toxicity has not been reported in other glyoxylate oxidoreductase-containing plants treated with glyphosate.

In conclusion, our work shows that evolved GO may be a novel system for the development of glyphosate-tolerant transgenic plants and may represent an effective supplement or alternative to the transgene currently being used that is based on an EPSPs insensitive to inhibition by glyphosate. The k_{cat}/K_m of G51S/A54R/H244A GO enzyme for glyphosate is $\approx 2 \times 10^3$ M^{-1} s^{-1}, significantly lower than diffusion-limited maximal value (10^9 M^{-1} s^{-1}). Thus, despite the dramatic improvement in kinetic efficiency with glyphosate, GO is far from the limits of optimization.

Acknowledgments—We thank Beamlines BL14.2 of BESSY (Helmholtz-Zentrum Berlin and BESSY II) for diffraction data. We kindly acknowledge the help of Dr. Andrea Mele and Walter Panzeri (Politecnico di Milano) for mass spectrometry analysis of GO reaction on glyphosate.

REFERENCES

1. Job, V., Marcone, G. L., Pilone, M. S., and Pollegioni, L. (2002) *J. Biol. Chem.* **277,** 6985–6993
2. Job, V., Molla, G., Pilone, M. S., and Pollegioni, L. (2002) *Eur. J. Biochem.* **269,** 1456–1463
3. Settembre, E. C., Dorrestein, P. C., Park, J. H., Augustine, A. M., Begley, T. P., and Ealick, S. E. (2003) *Biochemistry* **42,** 2971–2981
4. Mörtl, M., Diederichs, K., Welte, W., Molla, G., Motteran, L., Andriolo, G., Pilone, M. S., and Pollegioni L. (2004) *J. Biol. Chem.* **279,** 29718–29727
5. Funke, T., Han, H., Healy-Fried, M. L., Fischer, M., and Schönbrunn, E. (2006) *Proc. Natl. Acad. Sci. U.S.A.* **103,** 13010–13015
6. Padgette, S. R., Kolacz, K. H., Delannay, X., Re, D. B., LaVallee, B. J., Tinius, C. N., Rhodes, W. K., Otero, Y. I., Barry, G. F., Eichholz, D. A., Peschke, V. M., Nida, D. L., Taylor, N. B., and Kishore, G. M. (1995) *Crop. Sci.* **35,** 1451–1461
7. Duke, S. O., and Powles, S. B. (2008) *Pest. Manag. Sci.* **64,** 319–325
8. Goldsbrough, P. B., Hatch, E. M., Huang, B., Kosinski, W. G., Dyer, W. E., Herrmann, K. M., and Weller, S. C. (1990) *Plant Sci.* **72,** 53–62
9. Castle, L. A., Siehl, D. L., Gorton, R., Patten, P. A., Chen, Y. H., Bertain, S., Cho, H. J., Duck, N., Wong, J., Liu, D., and Lassner, M. W. (2004) *Science* **304,** 1151–1154
10. Pline-Srnic, W. (2006) *Weed Technol.* **20,** 290–300
11. Siehl, D. L., Castle, L. A., Gorton, R., Chen, Y. H., Bertain, S., Cho, H. J., Keenan, R., Liu, D., and Lassner, M. W. (2005) *Pest Manag. Sci.* **61,** 235–240
12. Siehl, D. L., Castle, L. A., Gorton, R., and Keenan, R. J. (2007) *J. Biol. Chem.* **282,** 11446–11455
13. Boselli, A., Rosini, E., Marcone, G. L., Sacchi, S., Motteran, L., Pilone, M. S., Pollegioni, L., and Molla, G. (2007) *Biochimie* **89,** 1372–1380
14. Goodsell, D. S., Morris, G. M., and Olson, A. J. (1996) *J. Mol. Recognit.* **9,** 1–5

15. Schüttelkopf, A. W., and van Aalten, D. M. (2004) *Acta Crystallogr. D. Biol. Crystallogr.* **60,** 1355–1363
16. Pollegioni, L., Lorenzi, S., Rosini, E., Marcone, G. L., Molla, G., Verga, R., Cabri, W., and Pilone, M. S. (2005) *Protein Sci.* **14,** 3064–3076
17. Caldinelli, L., Iametti, S., Barbiroli, A., Bonomi, F., Fessas, D., Molla, G., Pilone, M. S., and Pollegioni, L. (2005) *J. Biol. Chem.* **280,** 22572–22581
18. Leslie, A. G. (2006) *Acta Crystallogr. D. Biol. Crystallogr.* **62,** 48–57
19. Collaborative Computational Project No. 4. (1994) *Acta Crystallogr. D. Biol. Crystallogr.* **50,** 760–763
20. Murshudov, G. N., Vagin, A. A., and Dodson, E. J. (1997) *Acta Crystallogr. D. Biol. Crystallogr.* **53,** 240–255
21. Emsley, P., and Cowtan, K. (2004) *Acta Crystallogr. D. Biol. Crystallogr.* **60,** 2126–2132
22. Laskowski, R. A., MacArthur, M. W., Moss, D. S., and Thornton, J. M. (1993) *J. Appl. Crystallogr.* **26,** 283–291
23. Wagner, M. A., Trickey, P., Chen, Z. W., Mathews, F. S., and Jorns, M. S. (2000) *Biochemistry* **39,** 8813–8824
24. Hoagland, R. E. (1980) *Weed Sci.* **28,** 393–400
25. Reddy, K. N., Rimando, A. M., and Duke, S. O. (2004) *WSSA Abstr.* **44,** 116
26. DeLano, W. (2002) *PyMOL*, DeLano Scientific, San Carlos, CA